DOI: 10.7860/JCDR/2023/60751.17863

Review Article

Radiology Section

Role of Cross-sectional Imaging in Evaluation of Parotid Gland Tumours: A Pictorial Review

ASHWINI GOVISETTY[1], KARTHIKKRISHNA RAMAKRISHNAN[2], VEERARAGHAVAN GUNASEKARAN[3], KOMALI JONNALAGADDA[4], R VIMAL CHANDER[5], PAARTHIPAN NATARAJAN[6]

ABSTRACT

Radiological evaluation of the parotid gland neoplasms is a major challenge for radiologists, due to the wide variety of imaging features and differential diagnosis. Though Ultrasonography (USG) combined with guided Fine Needle Aspiration Cytology (FNAC) is the primary diagnostic modality, Computed Tomography (CT) and Magnetic Resonance Imaging (MRI) play an important role in the evaluation of patients presenting with suspected neoplastic lesions of the parotid gland. Cross-sectional imaging data of seven patients were selected and reviewed in detail. CT and MRI imaging had been done on patients referred to Radiology Department for clinically suspected parotid tumours. All of them underwent surgical excision and histopathological examination postimaging. Benign tumours usually arise from superficial lobe and exhibit strong signal intensity on T2 weighted images with well-defined margins. Lobulated margins with T2 dark rim are characteristic of pleomorphic adenoma. Hyperdense lesion with cystic changes with occasional bilateralism favour Warthin's tumour. Most of the malignant parotid tumours involve deep lobe and appear as low signal lesion on T2 weighted imaging with ill-defined margins. Locally aggressive features like subcutaneous/deep infiltration strongly suggests malignancy. Cross-sectional imaging feature of carcinoma ex pleomorphic adenoma is variable from focally aggressive to totally aggressive tumourigenesis. Few malignant tumours like high-grade Mucoepidermoid Carcinoma (MEC) and Adenoid Cystic Carcinoma (AdCC) can show tendency towards perineural spread. Although histopathological examination is required for definitive diagnosis, few pathology-specific imaging findings on cross-sectional imaging can help in localising and characterising the parotid lesions and categorising innocuous benign from sinister malignant lesions and thus narrow down the differential diagnosis.

Keywords: Adenoid cystic carcinoma, Magnetic resonance imaging, Mucoepidermoid carcinoma, Parotid gland neoplasms, Pleomorphic adenoma, Warthin's tumour

INTRODUCTION

Parotid tumours affect 1 in 100,000 people representing 2-3% of tumours of head and neck and 80% of salivary gland tumours. Most of these are benign with Pleomorphic adenoma being the most common, while MEC is the most common malignant lesion [1]. Neoplasms of salivary glands in children are rare occurrences, however, the percentage of malignant neoplasms remain high in children in comparison to the adult population. About 35% of all parotid gland tumours in children are malignant [2]. For benign neoplasms, local excision or partial/lateral parotidectomy is the surgical procedure of choice whereas complete parotidectomy in done for malignant ones. Surgical resection of these tumours is a complicated procedure risking facial nerve injury [2]. FNAC can be inconclusive owing to improper choice of site and difficulty in accessing the deep lobe. Differentiation between benign and malignant palpable tumours may not be possible always by clinical examination only. Therefore, presurgical diagnostic imaging and planning is of vital importance [2].

Cross-sectional imaging is helpful:

a) To localise and characterise the parotid lesions.

b) To differentiate benign from malignant lesions,

c) To study the deeper extent of disease, not possible by USG

d) To help in the early diagnosis of small, but significant risk of malignant transformation in pre-existing parotid tumours.

e) For planning and carrying out image-guided cytology and biopsy, tumour staging, and mapping for preoperative planning [3].

f) It is also helpful in deciding lymph node dissection if involved, expediting treatment for malignant neoplasms, deferring surgical intervention in inflammatory disease and for presurgical patient education [2].

There may be considerable overlapping of imaging features between benign and malignant tumours of the parotid gland. However, certain key cross-sectional imaging features along with histopathological correlation discussed in this article such as diffuse growth pattern/deep infiltration and perineural spread may help for early diagnosis of malignant tumours and appropriate management of the same.

Radiological Image Acquisition Parameters

Cross-sectional imaging data of seven patients were selected and reviewed in detail. CT and MRI imaging had been done on patients referred to Radiology Department for clinically suspected parotid tumours. All of them underwent surgical excision and histopathological examination postimaging. After obtaining necessary consent, CT or MRI of the neck spanning from the skull base to the apex of the lung was performed.

CT imaging was performed with PHILIPS INGENUITY 128 slice CT machine with following imaging parameters: Tube current 250 mA, 120 kV, collimation 128 x 0.625, pitch 0.993, rotation time 0.75 s/rotation, and acquisition slice thickness of 2 mm. Initially, Non Contrast Computed tomography (NCCT) was obtained throughout the entire neck and 1.5-2.0 mL/kg of low-osmolar non ionic contrast media (300 mg of iodine per milliliter) was injected by use of a power injector. Arterial phase scan was acquired at 25sec after contrast agent injection and the porto-venous phase scan was obtained at 60sec.

A 1.5T MRI unit (PHILIPS MULTIVA) with a neck coil was used for MRI. MR neck imaging protocol included the following sequences spanning the skull base to lung apex [Table/Fig-1]. Contrast MRI was done by injecting 0.2 mL/kg of Gadobutrol (Gd) (1.0 mmol/ml) contrast media.

Parameters	Sequences					
	Coronal T1	Axial T2	Axial T2 STIR	DWI	Post Gd T1 FS axial	Post Gd T1 FS coronal
TR (ms)	650	2500	3430	3417	641	617
TE (ms)	10	85	68	69	15	12
Section thickness (mm)	4	4	4	3	4	4.5
FOV (mm)	220x199	200x186	220x200	245x225	200x180	218x203
Resolution (mm)	244x179	224x157	220x164	112x114	200x132	220 x143
Voxed Size (mm)	0.9x1.1x4	0.9x1.1x4	1x1.3x4	2x2x3	0.9x1.1x4	1.0x1.4x4.5

[Table/Fig-1]: MR Imaging (MRI) sequences and their parameters.
TR: Repetition time; TE: Time to echo; FOV: Field of view; ms: Milliseconds; mm: Millimeter

DISCUSSION

1. Pleomorphic Adenoma

Pleomorphic adenoma is the most common benign salivary neoplasm in adults. It is also referred to as a "benign mixed tumour" due to the multifaceted origin and mixed histology reflecting myriad radiological findings. They may contain glandular, ductal, or solid types of epithelial elements originating from the intercalated duct myoepithelial cell unit. They also contain chondroid and fibromyxoid mesenchymal-like tissue. Areas of necrosis, haemorrhage, hyalinisation, calcification, and rarely, ossification may be present. Imaging findings vary depending on the tumour size. Despite multifaceted histopathological appearance as described most of the smaller-sized tumours are more homogeneous in appearance however, larger tumours have a non homogeneous appearance with sites of low attenuation representing areas of necrosis, old haemorrhage, and cystic changes [4]. MRI features described by Som PM and Brandwein-Gensler MS include a low T1-weighted and high T2-weighted signal intensity. A low-signal-intensity "capsule" is often seen on T2-weighted scans and fat-suppressed, contrast-enhanced, T1-weighted images [4]. Our patient's (a 32-year-old female with insidious onset, slowly progressive swelling in left parotid region) MR images showed a homogeneously enhancing, well-defined, T1 homogenous iso to hypointense, T2 homogeneous hyperintense mass lesion with lobulated sharp margins involving the superficial lobe with no diffusion restriction. A thin rim of T2 hypointensity representing 'capsule' was also seen in the periphery of the lesion. High probability MRI criteria for the diagnosis of pleomorphic adenoma described by Zaghi S et al., include bright signal on T2 weighted images, sharp margins, heterogeneous nodular enhancement, lobulated contours, T2-dark rim [5]. Our patient fulfilled these criteria except for homogeneous enhancement which is one of the neutral criteria for the diagnosis of pleomorphic adenoma. Histopathological correlation showed epithelial cells forming tubules, myoepithelial cells and chondromyxoid matrix [Table/Fig-2]. However, when large, these tumours usually have a non homogeneous, low to intermediate T1-weighted, and intermediate to high T2-weighted signal intensity. Areas of haemorrhage appear as regions of high signal intensity on both T1-weighted and T2-weighted images. Regions of necrosis usually have low T1-weighted and high T2-weighted signal intensity [4].

2. Carcinoma Ex-pleomorphic Adenomas

Carcinoma ex-pleomorphic adenomas are thought to arise from pre-existing pleomorphic adenomas. An inhomogeneous pattern is seen in larger pleomorphic adenomas, whereas hypointensity on T2-weighted images may be observed in carcinoma ex-pleomorphic adenomas [4]. Som PM and Brandwein-Gensler MS described the variable presentation of carcinoma ex pleomorphic adenoma on CT- it can simulate a huge pleomorphic adenoma with no obvious features suggesting malignancy. It may be a predominantly benign mixed tumour with a focal area of aggressive tumourigenesis presenting as a necrotic core, with irregularly thick walls and margins showing infiltration. Lastly, the neoplasm may be totally aggressive, with no evidence of benign pleomorphic tissue [4]. Our patient's (a 72-year-old male with complaints of expanding painful left-sided soft tissue swelling of face for three months) CT images showed ill-defined heterogeneously enhancing heterodense lesions with irregular margins involving both superficial and deep lobes with central non enhancing necrotic areas. Tumour cells arranged in papillary and glandular patterns lined by pleomorphic nuclei were observed on histopathological correlation [Table/Fig-3].

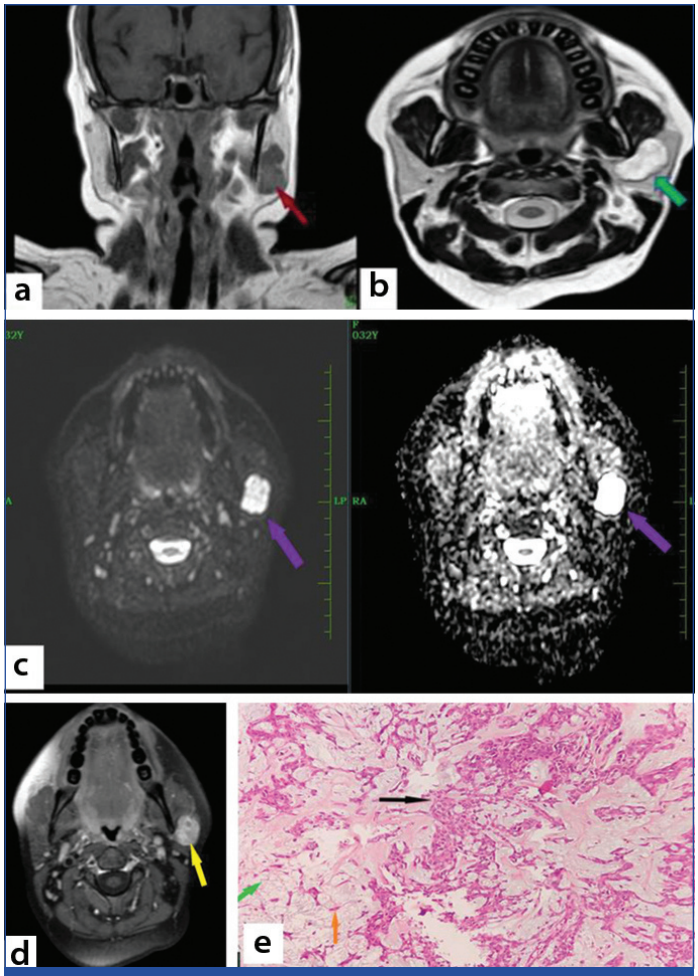

[Table/Fig-2]: On MRI: (a) a well-defined, T1 homogenous iso to hypointense; (b) T2 homogenous hyperintense lesion mass lesion with lobulated margins (red arrow) seen epicentered in superficial lobe of left parotid gland. Thin rim of T2 hypointensity representing 'capsule' seen in the posterior aspect (green arrow); (c) Postcontrast T1 fat suppressed images at the same level show near homogenous enhancement (yellow arrow); (d) On Diffusion Weighted Imaging (DWI), no diffusion restriction seen (violet arrows). With these imaging findings differentials of neoplastic lesions of parotid namely Pleomorphic adenoma and Warthin's tumour were given. This tumour turned out to be Pleomorphic adenoma on histopathology; (e) which showed epithelial cells forming tubules (black arrow), myoepithelial cells (orange arrow) and chondromyxoid matrix (green arrow).

3. Warthins' Tumour

Warthin's tumour (also known as cystadenolymphoma) is a benign salivary gland neoplasm representing about 2% to 15% of all primary epithelial tumours of the parotid gland and is the second most frequent benign neoplasm of the salivary glands after pleomorphic adenoma. In women, the peak incidence is in the 6th decade, whereas it is in the 7th decade in men. Warthin's tumour occasionally occurs in young patients [6]. Histopathological features of Warthin's tumour described by Limaiem F and Jain P include varying proportions of papillary cystic structures lined by oncocytic epithelial cells and a lymphoid stroma with germinal centres [6]. In a case report and review of literature, Naujoks C et al., described bilateralism as seen in 7-10% of the cases [7].

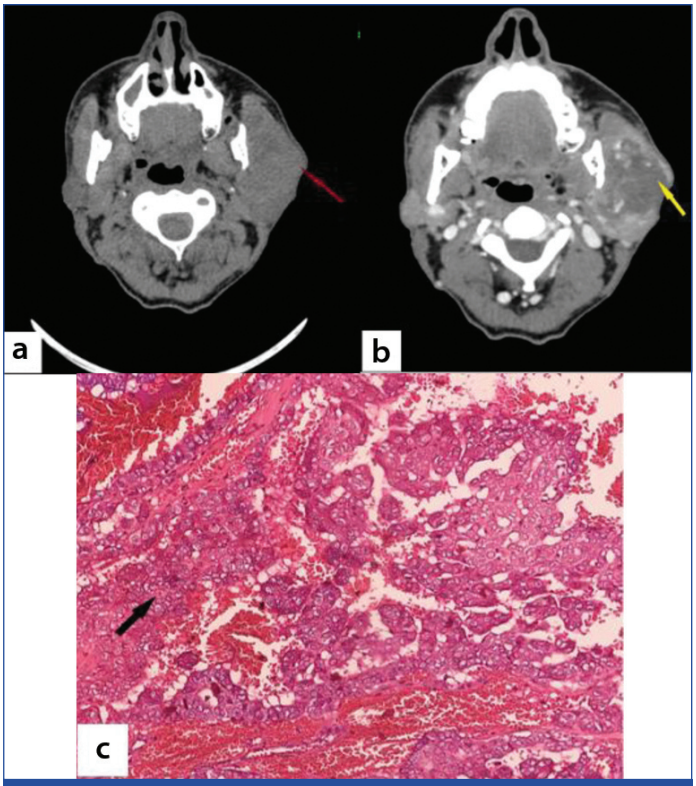

[Table/Fig-3]: (a) On Non Contrast Computed tomography (NCCT) an ill-defined heterodense lesion with irregular margins (red arrow) involving both superficial and deep lobes with; (b) postcontrast images showing heterogenous enhancement with central non enhancing necrotic area (yellow arrow); On Histopathology (c) tumour cells arranged in papillary and glandular pattern (black arrow) lined by pleomorphic nuclei was seen which was consistent with carcinoma ex pleomorphic adenoma.

CT features described by Som PM and Brandwein-Gensler MS include small, oval, homogeneous soft tissue density lesions, with smooth margins in the tail of the parotid with no dystrophic calcifications [8]. Among all parotid tumours, Warthin's tumour has the highest CT attenuation value on plain CT as described in a study conducted by Xu ZF et al., [9]. Cyst formation with homogenous material (+10 to 20 HU) is common. The cyst wall is usually thin and fairly smooth. The presence of a focal tumour nodule helps to distinguish Warthin's tumours with large cystic components, septae, or multiple adjacent cystic lesions from first branchial cleft cysts or lymphoepithelial cysts [8]. Our patient (a 71-year-old male, chronic smoker presented with painless swelling in lower portion of the right parotid region for four years) showed a well-defined, homogeneously enhancing smoothly marginated slightly hyperdense lesion on CT imaging with internal areas of hypoattenuation/cystic component which on histopathological examination showed a double layer of oncocytic cells resting on dense lymphoid stroma [Table/Fig-4]. Minami M et al., described the MRI features of Warthin's tumour which include low to intermediate signal intensity on T1 weighted images with few high signal intensity areas of cysts representing cholesterol crystals. Intermediate or mixed signal intensity exhibited on T2 weighted images represents abundant epithelial tissues while focal high signal intensity areas represent cysts or areas of predominant lymphoid proliferation [10]. Moderate signal intensity on Turbo Inversion Recovery Magnitude (TIRM) and low enhancement are also described on MRI in a study conducted by Christe A et al., to discriminate benign and malignant parotid tumours with lesion characteristics on MRI [11].

4. Parotid gland lipomas

Parotid gland lipomas are rare benign neoplastic lesions accounting for only 0.6% of benign parotid tumours. These are often involving the superficial lobe as slow-growing asymptomatic nodular masses. Without proper preoperative imaging, clinically it can mimic pleomorphic adenoma or Warthin's tumour due to the benign indolent nature of the lesion. Lipomas may exhibit CT density in

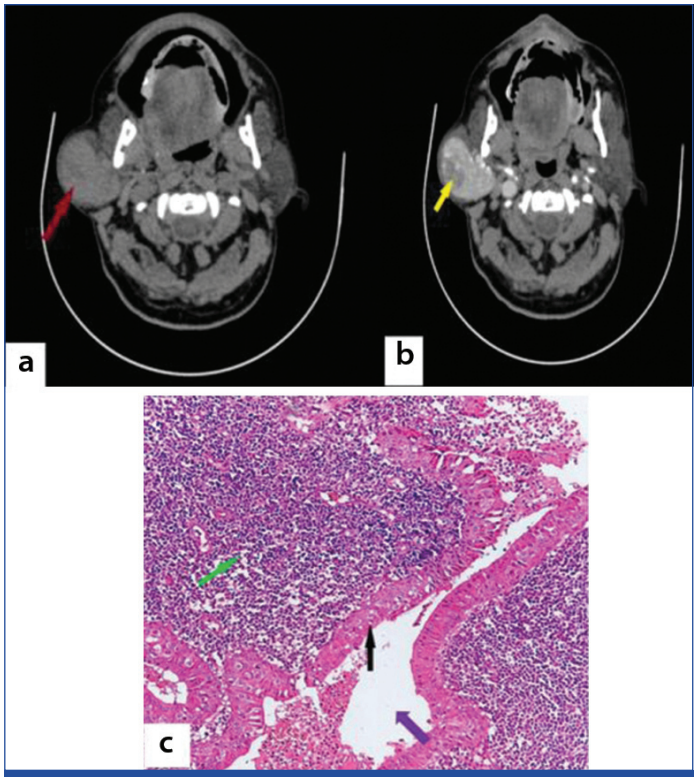

[Table/Fig-4]: (a) NCCT shows a well-defined smoothly marginated slightly hyperdense lesion with internal areas of hypoattenuation noted in the right parotid gland (red arrow); (b) Contrast enhanced CT image shows near homogenous enhancement with internal eccentric non-enhancing area likely cystic component (yellow arrow). With these imaging findings differentials of neoplastic lesions of parotid namely Pleomorphic adenoma and Warthin's tumour were given; (c) On Histopathology the tumour turned out to be Warthin's tumour showing double layer of oncocytic cells (black arrow) resting on dense lymphoid stroma (green arrow) with cystic changes (violet arrow).

the range between -150 to -50 Hounsfield Units [12]. Tong KN et al., classified the parotid gland lipomas based on the location and histologic subtypes: a) periparotid (lesions on the superficial surface of the gland); and b) intraparotid (lesions occurring within the parenchyma of the gland) as in our patient's CT (37-year-old female came with swelling and pain in right parotid region for a period of one month) [Table/Fig-5] [12]. Histopathologically, true lipomas are identified by thin fibrous capsule surrounding a mass of uniform-sized mature adipocytes, through which we can differentiate a few unencapsulated fat-containing lesions such as lipomatosis, pseudolipoma, and lobular lipomatous atrophy [12].

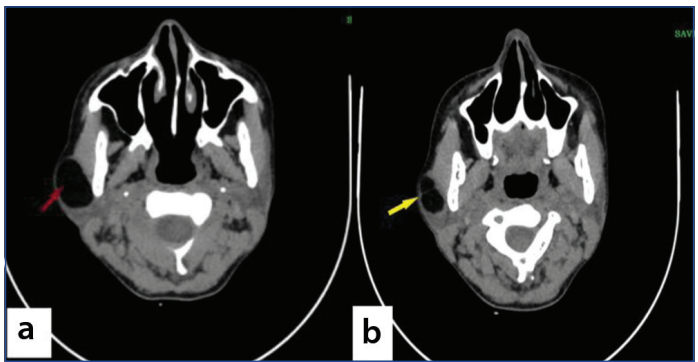

[Table/Fig-5]: (a,b) NCCT a well-defined hypodense lesion (red arrow) (mean HU -105 fatty attenuation) epicentered in the superficial lobe of right parotid gland, with few internal incomplete strands/septae (yellow arrow). With these imaging findings diagnosis of fat containing benign lesion of parotid namely lipoma was given.

5. Mucoepidermoid Carcinoma (MEC)

MEC is the most common malignancy of the salivary gland with more than 80% of the MECs occurring in the parotid gland [13]. Kashiwagi N et al., conducted a study to correlate MRI features of MEC with the histopathological features and classified MECs as high, intermediate, or low-grades based on the histological features correlating with the clinical behaviour of the tumours [13].

Pluripotent reserve cells of the excretory ducts are thought to be the cell of origin for MEC comprising three different cell types: mucinous, intermediate, and epidermoid. It may be difficult to differentiate the tumour grades by FNAC alone because of inadequate sampling, selection bias/errors, and the lack of objectivity. For proper surgical planning preoperative imaging has an important role with MRI findings being near congruent to the pathological grading.

a) **Low-grade MEC:** Due to the presence of abundant mucin-secreting cells, low-grade tumours usually exhibit hyperintense signals on T2-weighted images reflecting a cystic architectural pattern [13]. Our patient's (35-year-old female presented with painless right parotid swelling, insidious in onset for 2 years) MRI showed a well-defined homogeneously enhancing, T1 hypointense, and T2 heterogeneously hyperintense lesion along the superficial lobe of the right parotid gland with mild diffusion restriction with sheets of malignant cells composed predominantly of mucinous cells lining cystic and glandular spaces on histopathological examination [Table/Fig-6]. Even low-grade tumours may exhibit ill-defined margins due to peritumoural inflammatory changes, thus poor definition of tumour margins should not be the singular criteria to call for high-grade MECs.

b) **Intermediate-grade MECs:** These can show combined imaging features of low and high-grade MECs.

c) **High-grade MEC:** Due to the high-cellularity and invasive nature of the high-grade tumours, they often demonstrate low to intermediate signal intensities on T2 weighted images with ill-defined margins. Histopathologically, high-grade MEC usually demonstrate solid architectural pattern with predominant epidermoid or spindle-shaped cells with high nucleus-to-cytoplasm ratio [13].

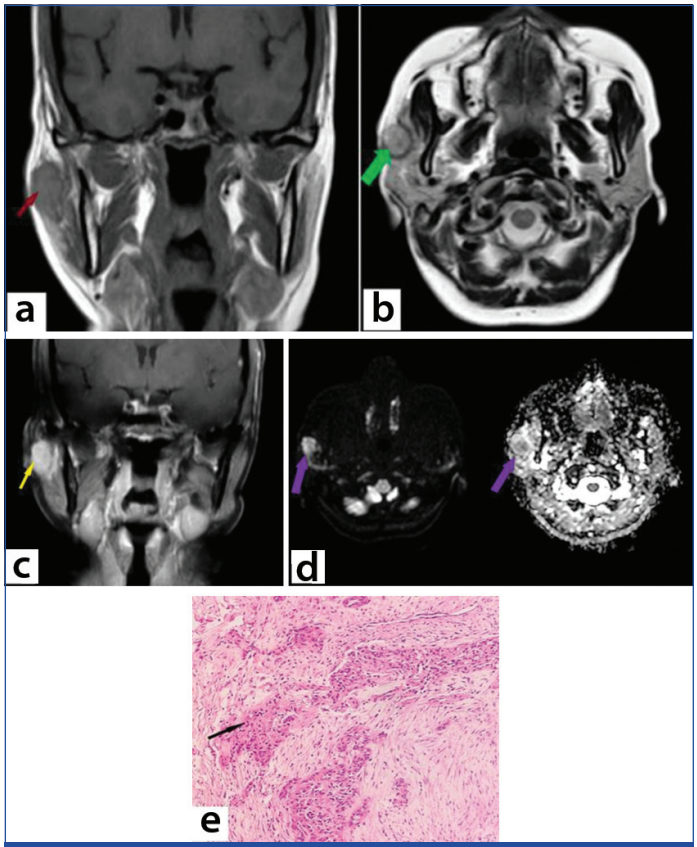

[Table/Fig-6]: (a) On MRI a well-defined T1 hypointense lesion (red arrow); and (b) T2 heterogeneously hyperintense (green arrow) lesion along the superficial lobe of right parotid gland; (c) Postcontrast T1 fat suppressed images at the same level show near homogenous enhancement (yellow arrow); (d) DWI showed diffusion restriction with reduced diffusivity in ADC (violet arrows). With these imaging findings differentials of neoplastic lesions of parotid namely atypical/degenerative Pleomorphic adenoma/early suspicious Mucoepidermoid Carcinoma (MEC) was given; (e) Histopathology the tumour turned out to be low-grade Mucoepidermoid Carcinoma (MEC) showing sheets of malignant cells composed predominantly of mucinous cells lining cystic and glandular spaces (black arrow).

A study conducted by Chandra P and Nath S, described the simultaneous perineural spread of MEC of parotid gland involving V, VI, and VII cranial nerves on Positron Emission Tomography/CT in 23% of patients and is of strong prognostic significance in MEC and has been linked with lower overall survival [14]. MRI of our patient (45-year-old female with complaints of painful enlarging mass in the left cheek for seven years with increasing in size over past two months) with high-grade MEC showed mixed signal intensity on T2W images with diffusion restriction with heterogeneous postcontrast enhancement with perineural spread along the branches of the mandibular nerve which on histopathological correlation showed solid sheets of malignant spindle shaped cells with nuclear pleomorphism and high nuclear-cytoplasm ratio with scarcity of mucoid cells suggestive of high-grade MEC [Table/Fig-7].

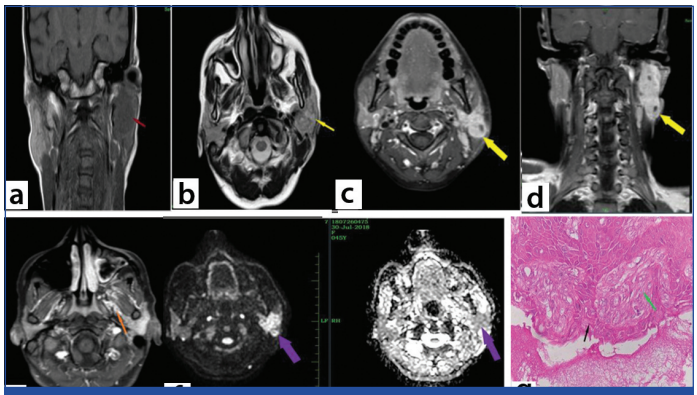

[Table/Fig-7]: (a) On MRI ill-defined T1 heterogeneous mixed signal intense lesion (red arrow) involving both superficial and deep parotid glands exhibiting; (b) T2 mixed signal changes with small cystic areas (yellow arrow) within; (c,d) Postcontrast T1 fat suppressed images show heterogeneous enhancement (yellow arrows); (e) Contrast enhancement noted along the branches of the anterior division of the left mandibular nerve (orange arrow); (f) DWI showed diffusion restriction with reduced diffusivity in ADC (violet arrows). With these imaging findings differentials of neoplastic malignant aetiology like Mucoepidermoid Carcinoma (MEC)/adenoid cystic carcinoma were given in view of perineural involvement; On Histopathology (g) the tumour turned out to be high-grade Mucoepidermoid Carcinoma (MEC) showing solid sheets of malignant spindle shaped cells (black arrow) with nuclear pleomorphism and high nuclear-cytoplasm ratio. Few mucoid cells (green arrow) are also noted.

6. Adenoid Cystic Carcinoma (AdCC)

Adenoid Cystic Carcinoma (AdCC) accounts for 2% to 6% of parotid neoplasia and occurs over a very wide age range, from the first to the ninth decades of life, but with a peak incidence in the fourth to seventh decades. The female-to-male ratio is approximately 3:2. It is a slow-growing, widely infiltrative tumour with a tendency toward perineural spread [15]. AdCC can exhibit either benign or malignant behaviour on cross-sectional imaging as described by Som PM and Brandwein-Gensler MS [15]. Most of the parotid gland AdCC tend to exhibit benign morphology, whereas the minor salivary gland AdCC may turn out to be malignant [15]. Histopathologically, AdCC is composed of a mixture of epithelial and ductal cells which are arranged in three characteristic patterns-cribriform, tubular, and solid as described by Godge P et al., with most tumours being composed of a mix of these [16]. They also graded AdCC histologically as follows: a) Grade-I: The tumour consists only of cribriform and tubular histomorphology; b) Grade-II: A mixture of cribriform, tubular, and solid growth patterns, with solid growth patterns less than 30% of the tumour; c) Grade-III: Tumours with predominantly solid features (>30% or more of the tumour). The relationship between histological pattern and prognosis of AdCC has been studied. Overall survival rates of 16.7% after a 10-year treatment for cases where the solid variable was observed and 47.4% for lesions where cribriform and tubular standards [16]. Ouatassi N et al., described the MRI features of AdCCas they can either appear as a defined mass or an ill-defined mass with diffuse infiltration of its surrounding structures with homogeneous enhancement on post-gadolinium images. However, heterogeneous enhancement

may be noticed in tumours with areas of necrosis. The solid and more cellular histological subtype of AdCC has a lower signal on T2-weighted MRI. Irregular margins, adjacent tissue infiltration, and hypo intensity in T2-weighted sequences are characteristic of malignant tumours, respectively with decreasing predictive value [17]. Our patient's (46-year-old female who presented with painless swelling in righ-side of the face since seven months with rapid increase in size over past one month) MRI showed a heterogeneously enhancing, T2 intermediate signal intensity lesion predominantly involving the superficial lobe with a central non enhancing necrotic component with peripheral diffusion restriction and cribriform and tubular architecture on histopathological examination [Table/Fig-8]. Som PM and Brandwein-Gensler MS also described the perineural invasion of the skull base often occurs via the facial nerve or the mandibular nerve. Perineural invasion is consistently and more reliably identified on MRI than CT. Widening of the bony neural canal representing enlarged nerve and obliteration of normal fat present at the extracranial opening of these canals can be identified on contrast-enhanced CT [15]. However, lesser degrees of neural invasion of the tumour can reliably be identified by MRI by nerve enhancement even in a minimally enlarged nerve [15]. Our patient did not show any signs of perineural invasion on MRI which may be due to the earlier clinical presentation.

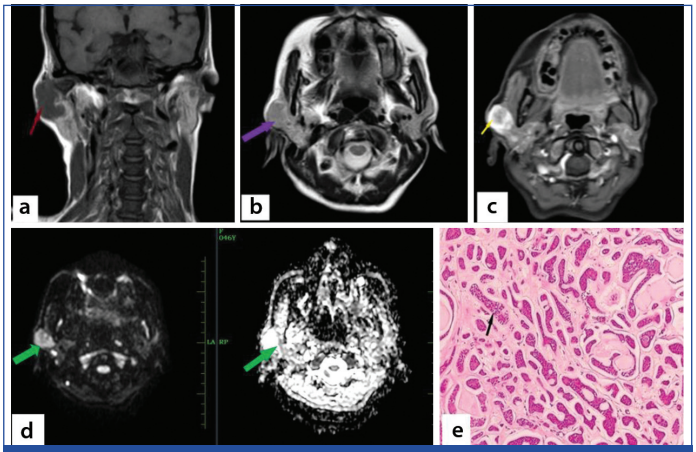

[Table/Fig-8]: (a) A fairly defined lesion T1 hypointense (red arrow) and T2 intermediate; (b) signal intensity (violet arrow) lesion in the right parotid region predominantly involving the superficial lobe; (c) Postcontrast T1 fat suppressed images at the same level shows heterogenous enhancement with central non-enhancing necrotic component (yellow arrow); (d) DWI image shows peripheral diffusion restriction (green arrows). With these imaging findings differentials of neoplastic malignant aetiology like Mucoepidermoid Carcinoma (MEC)/adenoid cystic carcinoma were given; On histopathology (e) showed tumour cells arranged in cribriform and tubular architecture (black arrow) in consistent with a low-grade variant of adenoid cystic carcinoma.

Characteristic MRI findings used to distinguish benign and malignant tumours are described in [Table/Fig-9].

MRI findings	Benign	Malignant
T2W Images	Strong signal intensity	Low signal intensity
Margins after contrast administration	Well-defined	Ill-defined
Most commonly arise from	Superficial lobe	Deep lobe/both
Perineural spread, subcutaneous infiltration	Absent	Present

[Table/Fig-9]: MR Imaging (MRI) findings (benign versus malignant lesions).

Typical cross-sectional imaging findings for the most frequently encountered parotid tumours are described in [Table/Fig-10]. Major limitations of this review include a small number of patients cross-sectional imaging was done in the hospital, and MRI was not done in few of patients due to the poor socio-economic status. And further MRI was not warranted in one patient diagnosed with Warthin's tumour due to the characteristic CT findings as described. Surgical excision/histopathological examination was not done in the patient with parotid lipoma due to the benign imaging features and due to functional/aesthetic concerns.

Tumour	Appearance
Pleomorphic adenoma	1. High signal intensity on T2W images. 2. Strong enhancement. 3. Defined borders. 4. Lobulated margin. 5. Most common location: Superficial lobe.
Carcinoma-ex-pleomorphic adenoma	1. Low signal intensity on T2-weighted images. 2. One of the following several CT appearances: a) It can simulate a huge pleomorphic adenoma with no obvious features suggesting malignancy. b) It may be predominantly benign mixed tumour with focal area of aggressive tumourigenesis presenting as a necrotic core, with irregularly thick walls and margins showing infiltration. c) It may be totally aggressive, with no evidence of a benign pleomorphic tissue
Lipoma	Well-defined, non enhancing, hypodense/fat density (-150 to -50 HU) lesion
Warthin's tumour	1. Hyperdense on CT. 2. Cystic changes+ 3. Moderate signal intensity on TIRM 4. Low enhancement
Mucoepidermoid Carcinoma	Low-grade tumours: High signal intensity on T2W images. High-grade tumours: Low-intermediate signal intensity. Ill-defined margins: High-grade >> Low-grade. Perineural spread may occur
Adenoid cystic carcinoma	Cribriform/tubular morphology: T2 isointense Mixed morphology with solid components: T2 hypointense Diffuse growth pattern with perineural spread.

[Table/Fig-10]: Typical cross-sectional imaging findings for the most frequently encountered parotid tumours.

CONCLUSION(S)

Even though various parotid neoplastic lesions present with similar clinical features, and history, they have varied radiological presentations, clinical courses, and histopathological features. Therefore, preoperative evaluation to arrive at an accurate presurgical imaging diagnosis is exacting and vital. Cross-sectional imaging plays an important role in characterising the lesions, helping to narrow down the differential diagnoses to arrive at a provisional diagnosis nearest to the histopathological diagnosis. MRI is superior to CT in assessing the extent of the tumour and invasion of neighboring structures and perineural spread.

Acknowledgement

The authors express their sincere gratitude to all the patients and their relatives for consenting to be part of this review and to Professor Dr. Seena C.R, Senior Consultant and Professor of Radiology for her invaluable support and guidance.

Authors contributions: AG contributed to the conception and design, data acquisition, literature search and manuscript drafting. VG contributed to the literature search, manuscript drafting, editing and revision. KKR contributed to the conception and design, literature search, manuscript drafting, editing and revision. PN contributed to revision and approval of final draft. All authors approved the final version to be published.

REFERENCES

[1] Maahs GS, Oppermann Pde O, Maahs LG, Machado Filho G, Ronchi AD. Parotid gland tumours: A retrospective study of 154 patients. Braz J Otorhinolaryngol. 2015;81(3):301-06. Doi: 10.1016/j.bjorl.2015.03.007.
[2] Thoeny HC. Imaging of salivary gland tumours. Cancer Imaging. 2007;7(1):52-62. Doi: 10.1102/1470-7330.2007.0008.
[3] Mittal S, Vinayak V, Grover S, Kumar M. Imaging criteria for salivary gland tumours-an overview. Indian Journal of Contemporary Dentistry. 2013;1(1):18. https://dx.doi.org/10.5958/j.2320-5962.1.1.005.

[4] Som PM, Brandwein-Gensler MS. Salivary Glands: Anatomy and Pathology, Pleomorphic adenoma. In: Som PM, Curtin HD, editors. Head and Neck Imaging. 5th ed. St. Louis: Mosby; 2011. Pp. 2525-35.
[5] Zaghi S, Hendizadeh L, Hung T, Farahvar S, Abemayor E, Sepahdari AR. MRI criteria for the diagnosis of pleomorphic adenoma: a validation study. American Journal of Otolaryngology. 2014;35(6):713-18.
[6] Limaiem F, Jain P. Warthin Tumour. [Updated 2022 Apr 30]. In: StatPearls [Internet]. Treasure Island (FL): StatPearls Publishing; 2022 Jan-. Available from: https://www.ncbi.nlm.nih.gov/books/NBK557640/
[7] Naujoks C, Sproll C, Singh DD, Heikaus S, Depprich R, Kübler NR, et al. Bilateral multifocal Warthin's's tumours in upper neck lymph nodes. Report of a case and brief review of the literature. Head & Face Medicine. 2012;8(1):01-06.
[8] Som PM, Brandwein-Gensler MS. Salivary Glands: Anatomy and Pathology, Warthin's's tumour. In: Som PM, Curtin HD, editors. Head and Neck Imaging. 5th ed. St. Louis: Mosby; 2011. Pp. 2535-44.
[9] Xu ZF, Yong F, Yu T, Chen YY, Gao Q, Zhou T, et al. Different histological subtypes of parotid gland tumours: CT findings and diagnostic strategy. World J. Radiol. 2013;5(8):313.
[10] Minami M, Tanioka H, Oyama K, Itai Y, Eguchi M, Yoshikawa K, et al. Warthin's tumour of the parotid gland: MR-pathologic correlation. AJNR Am J Neuroradiol. 1993;14(1):209-14.
[11] Christe A, Waldherr C, Hallett R, Zbaeren P, Thoeny H. MR imaging of parotid tumours: typical lesion characteristics in MR imaging improve discrimination between benign and malignant disease. AJNR Am J Neuroradiol. 2011;32(7):1202-07.
[12] Tong KN, Seltzer S, Castle JT. Lipoma of the parotid gland. Head Neck Pathol. 2020;14(1):220-23. Doi: 10.1007/s12105-019-01023-3. Epub 2019 Mar 19.
[13] Kashiwagi N, Dote K, Kawano K, Tomita Y, Murakami T, Nakanishi K, et al. MRI findings of mucoepidermoid carcinoma of the parotid gland: correlation with pathological features. Br J Radiol. 2012;85(1014):709-13.
[14] Chandra P, Nath S. Perineural spread of mucoepidermoid carcinoma of parotid gland involving V, VI, and VII cranial nerves demonstrated on positron emission tomography/computed tomography. Indian J Nucl Med. 2017;32(3):245-46.
[15] Som PM, Brandwein-Gensler MS. Salivary Glands: Anatomy and Pathology, Adenoid cystic carcinoma. In: Som PM, Curtin HD, editors. Head and Neck Imaging. 5th ed. St. Louis: Mosby; 2011. Pp. 2557-62.
[16] Godge P, Sharma S, Yadav M. Adenoid cystic carcinoma of the parotid gland. Contemp Clin Dent. 2012;3(2):223-26.
[17] Ouatassi N, Elguerch W, Bensalah A, Maaroufi M, Alami MN. Unusual presentation of parotid gland adenoid cystic carcinoma: A case presentation and literature review. Radiology Case Reports. 2022;17(2):344-49.

PARTICULARS OF CONTRIBUTORS:
1. Consultant Radiologist, Department of Radiodiagnosis, Aarthi Scans and Labs, Bengaluru, Karnataka, India.
2. Assistant Professor, Department of Radiodiagnosis, Saveetha Medical College and Hospital, Chennai, Tamil Nadu, India.
3. Assistant Professor, Department of Radiodiagnosis, Saveetha Medical College and Hospital, Chennai, Tamil Nadu, India.
4. Postgraduate Resident, Department of Radiodiagnosis, Saveetha Medical College and Hospital, Chennai, Tamil Nadu, India.
5. Associate Professor, Department of Pathology, Saveetha Medical College and Hospital, Chennai, Tamil Nadu, India.
6. Professor and Head, Department of Radiodiagnosis, Saveetha Medical College and Hospital, Chennai, Tamil Nadu, India.

NAME, ADDRESS, E-MAIL ID OF THE CORRESPONDING AUTHOR:
Veeraraghavan Gunasekaran,
Assistant Professor, Department of Radiodiagnosis,
Saveetha Medical College and Hospital, Chennai, Tamil Nadu, India.
E-mail: dr.gveeraraghavan@gmail.com

PLAGIARISM CHECKING METHODS: [Jain H et al.]
- Plagiarism X-checker: Oct 17, 2022
- Manual Googling: Dec 15, 2022
- iThenticate Software: Jan 20, 2023 (23%)

ETYMOLOGY: Author Origin

AUTHOR DECLARATION:
- Financial or Other Competing Interests: None
- Was informed consent obtained from the subjects involved in the study? Yes
- For any images presented appropriate consent has been obtained from the subjects. Yes

Date of Submission: **Oct 17, 2022**
Date of Peer Review: **Dec 01, 2022**
Date of Acceptance: **Jan 21, 2023**
Date of Publishing: **Apr 01, 2023**